Nuclear Engineering and Technology xxx (xxxx) xxx

Contents lists available at ScienceDirect

Nuclear Engineering and Technology

journal homepage: www.elsevier.com/locate/net

Original Article

Radiation doses assessment and radon exhalation rate from the soils of Albyda area, Yemen

Mohamed Y. Hanfi [a,b,*], Hany El-Gamal [c], Maher Taher Hussien [d], Mayeen Uddin Khandaker [e,f,j,**], Mohammed S. Alqahtani [g,h], Mohamed Hasabelnaby [i]

[a] Nuclear Materials Authority, P.O. Box 530, Maadi, Egypt
[b] Ural Federal University, Mira street19, 620002, Ekaterinburg, Russia
[c] Technology of Radiology and Medical Imaging Department, Faculty of Applied Health Sciences Technology, Menoufia University, 32951, Menoufia, Egypt
[d] Physics Department, Faculty of Education Yafea, Aden University, Aden, Yemen
[e] Applied Physics and Radiation Technologies Group, CCDCU, School of Engineering and Technology, Sunway University, Bandar Sunway, Selangor, 47500, Malaysia
[f] Faculty of Graduate Studies, Daffodil International University, Daffodil Smart City, Birulia, Savar, Dhaka, 1216, Bangladesh
[g] Central Labs, King Khalid University, Al Qura'a, P.O. Box 960, Abha, Saudi Arabia
[h] Radiological Sciences Department, College of Applied Medical Sciences, King Khalid University, Abha, 61421, Saudi Arabia
[i] Radiology and Medical Imaging Technology Department, School of Technology of Applied Health Sciences, Badr University in Cairo, 11829, Cairo, Egypt
[j] Department of Physics, College of Science, Korea University, 145 Anam-ro, Seongbuk-gu, Seoul, 02841, Republic of Korea

A R T I C L E I N F O

Keywords:
Soil
Radionuclides concentration
Alpha GUARD
Dose rate
Radon exhalation rate

A B S T R A C T

This work focuses on evaluating the potential health hazards posed by natural radionuclides in soil samples collected from 20 different sites in the Albyda area, Yemen. The activity concentrations of ^{226}Ra, ^{232}Th and ^{40}K and radon exhalation rates in the soil samples were investigated. Alpha GUARD detector was used to estimate ^{222}Rn concentration, while activity levels for natural radionuclides were measured by HPGe detector. The average values obtained for ^{226}Ra, ^{232}Th, and ^{40}K were 27.60 ± 2.40 Bq/kg, 35.07 ± 2.45 Bq/kg, and 544.71 ± 48 Bq/kg, respectively, and for ^{222}Rn concentrations were 135 ± 15 Bq/m^3. Our findings show that the concentrations of radionuclides were within the limits of the world average established by UNSCEAR, except the concentrations of ^{40}K, which was slightly higher than the world average (420 Bq/kg), while the average ^{222}Rn concentration was lower than the ICRP reference level of 300 Bq/m^3, and the average area exhalation rate 3.46 $\times 10^{-5}$ Bq m^{-2} s^{-1} was lower than the UNSCEAR world average of 0.016 Bq m^{-2} s^{-1}. Therefore, the soil in this study does not pose any radiological hazard to the population due to the harmful effects of ionizing radiation. The results of the current study highlight the potential health hazard posed by radon and radioactivity levels in the soil samples from Albyda area, Yemen, which will help to increase awareness of the radiological hazard and the data could also be used as a reference for future research on radioactivity mapping in the study area.

1. Introduction

Primordial radionuclides such as radium, thorium, and potassium, along with their daughter gas radon, are widely distributed in the Earth's crust. Most of the radioactivity in soils comes from the radioactive decay of ^{238}U (55.8 %), ^{232}Th (14.8 %), and ^{40}K (13.8 %). Natural radiation accounts for the majority of the world's radiation exposure [1–3]. The two main ways in which humans are exposed to natural radiation are through the external pathway, which results from gamma emission, and the internal pathway, which results in part from radon gas and its decay products, which are alpha particle emitters [4–7].

^{222}Rn is radioactive gas that occurs naturally in the Earth's crust as a result of the alpha decay of ^{226}Ra, a component of the ^{238}U decay series [8–10]. Most human exposure to (^{222}Rn) comes from the soils and rocks underneath buildings [11–13], variety of factors can affect the amount of radon in the soil, including soil types, climatic conditions, and weather patterns [14,15]. Radon has become a potential threat to human health because it has a density greater than that of air and can penetrate rock, soil, and basements, as well as water supplies from wells due to its substantial solubility in water. Radon decay products such as

* Corresponding author. Nuclear Materials Authority, P.O. Box 530, Maadi, Egypt.
** Corresponding author. School of Engineering and Technology, Sunway University, Subang Jaya, Selangor, 47500, Malaysia.
E-mail addresses: mokhamed.khanfi@urfu.ru (M.Y. Hanfi), mayeenk@sunway.edu.my (M.U. Khandaker).

https://doi.org/10.1016/j.net.2024.09.030
Received 7 May 2024; Received in revised form 4 August 2024; Accepted 23 September 2024
Available online 7 October 2024

^{218}Po, ^{214}Bi, and ^{214}Pb can enter the body through ingestion of contaminated well water or absorption into dust particles and then be inhaled into the lungs [16,17].

There are three processes by which radon can escape from soil and enter the atmosphere [9,11,18,19]. Initially, radon atoms were emitted into the pore space between the grains as a result of the decay of radium released from the grains. The radon emission coefficient is the fraction of radon atoms released from radium-bearing grains into the intergranular space as a result of radium decay. The second step is the movement, diffusion, and convection of radon atoms from the grains to the soil surface through the soil matrix, and the final step is the exhalation of radon atoms that move to the soil surface into the atmosphere.

Radon atoms have poor diffusion characteristics within solid materials, which means that they are difficult to release into the atmosphere

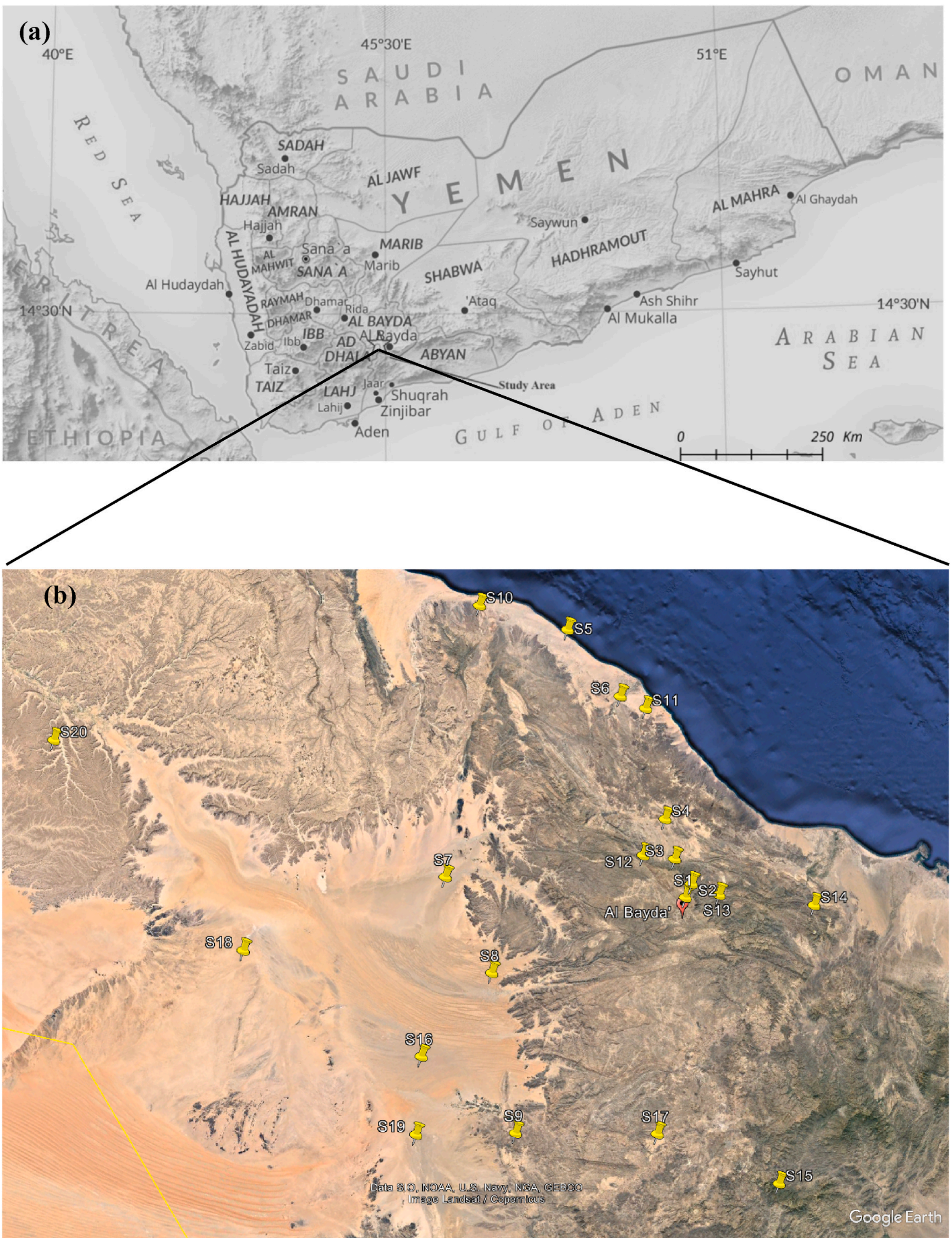

Fig. 1. (a) Location study of area, (b) the distribution of soil samples.

when contained within solid grains [20,21]. On the other hand, the gases can be completely dispersed in the top layer of soil and enter the atmosphere as soil gas if they are found in the spaces between the soil particles. Radon is more than 7.5 times denser than air and more than 100 times denser than hydrogen, so it tends to be found in lower areas of the home and basement. Radon is present in the atmosphere near the ground due to seepage from soil and rock [22,23].

Studies have shown a significant association between high levels of radon gas in residential areas and an increased risk of developing lung cancer. Radon's short-lived decay products can become trapped in lung tissue, releasing alpha particle energies that contribute to the development of radiogenic lung cancer [24–27]. In fact, research has identified radioactive radon gas as the second most significant contributor to the development of lung cancer., following closely behind tobacco smoking [28,29] Therefore, it is crucial to accurately assess radon concentration levels to evaluate the radiological hazards from this gas. The primary objective of this investigation is:

1 To measure and evaluate natural radioactivity levels and radon exhalation rates in soil samples from the Al-Baydha region of Yemen.
2 To assess the possible threat to the local population and environment from radioactive contamination, we measure the radon ^{222}Rn exhalation rates and analyze the concentrations of radionuclides such as ^{40}K, ^{232}Th, and ^{226}Ra.
3 To ensure public safety and guide the safe use of these soils in construction and agriculture, this research provides critical baseline data for the radiological characterization of the area. The results will serve as a reference for future research and radiological mapping initiatives in Yemen, furthering our understanding of naturally occurring radioactive materials (NORM) and their impacts.

2. Material and methods

2.1. Study area and geological setting

The governorate of Al-Baydha is located in the center of Yemen, about 267 km south of Sana'a, at an elevation above sea level. With a total of 20 districts, the capital of the governorate is the city of Al-Baydha, located at a latitude of 13.9889146 and a longitude of 45.5771002. Al-Baydha shares its borders with eight other governorates in Yemen, the Ma'rib and Shabwa governorates from the north, and parts of the Shabwa and Abyan governorates from the east. Parts of Abyan, Lahj, and Al Dhalea governorates from the south, and parts of Al Dhalea, Ibb, and Dhamar governorates from the west. Fig. 1 shows a location map of the study area. The Republic of Yemen is located in the southern region of the Arabian Peninsula. The land of Yemen is predominantly rocky, with rocks that date back to before the Cambrian era. Some of these Cambrian rocks are even older, dating back to about 3 billion years ago. Geologically, Yemen is part of the Arabian Shield. The main occupation of the residents of the governorate is agriculture, with the governorate contributing 6.4 % of the total agricultural output of the republic. The main crops grown include vegetables and cash crops, along with some handicrafts and traditional industries.

2.2. Samples preparation

Surface soil samples were collected from various locations within the study area using a stainless steel sampler at a depth of 0–5 cm. To obtain the desired size enriched in heavy minerals, the samples were crushed and passed through a 1 mm mesh. To eliminate any significant moisture, all samples go through an oven at 110 °C for 24 h. The weighed samples were placed in cylindrical polyethylene beakers, these beakers were well sealed to stop the leakage of ^{222}Rn from the samples. The beakers were stored for four weeks to ensure the establishment of a stable equilibrium between radium, thorium and their respective decay products [30].

2.3. Radioactivity measurement

All samples collected for gamma spectrometry were analyzed using an HPGe detector (Canberra, model GR4020) with a relative efficiency of 40 % for a 3″ × 3″ NaI (Tl) detector and an energy resolution of 2 keV at the 1332 keV gamma of ^{60}Co. Sample analysis was performed at the Nuclear Physics Laboratory, Department of Physics, Faculty of Science, Assiut University, Egypt. The lead well that housed the detector was shielded with a 6.22 cm thickness and internally lined with a 0.6 mm carbon composite. A spectroscopy amplifier (Canberra, model 2002CSL) was connected to the detector output. The point sources of ^{133}Ba, ^{60}Co, ^{137}Cs, ^{54}Mn, ^{22}Na and ^{65}Zn were used for the energy calibration of the system, the calibration was facilitated by the LabSOCSs (Laboratory Source less Calibration Software) installed in the spectrometer. Genie 2000 software from Canberra, USA was used for spectral analysis. The measurement duration was set to 28800 s for both activity and background. The radionuclides ^{226}Ra were determined from the gamma peak of ^{214}Pb (351.9 keV) and the 609.3 keV, 1120.3 keV, and 1764 keV gamma peaks of ^{214}Bi. The estimate of ^{232}Th was made from a gamma peak of ^{228}Ac 911.2 keV, a gamma peak of ^{212}Pb 238.6 keV, and the 2614 keV gamma ray from ^{208}Tl. Finally, ^{40}K levels were determined from the 1461 keV gamma peak. The activity concentration (S) values for the ^{226}Ra, ^{232}Th series and ^{40}K found in the samples can be calculated from the equation [31]:

$$S\ (Bq/kg) = \frac{C_n}{t_c \times I\gamma\ (E\gamma) \times \varepsilon\ (E\gamma) \times M} \quad (1)$$

Where then number of energy peaks after background subtraction is denoted as C_n, where t_c is the time of measurement (second), $I\gamma$ ($E\gamma$) is the probability of gamma rays emitted at energy $E\gamma$, while ε ($E\gamma$) is the absolute detector efficiency at energy $E\gamma$. Finally, M is the mass of the sample to be measured (kg).

2.4. Radiological health risks assessment

Radium equivalent activity (Ra_{eq}) is a specified index used to compare the individual radioactivity of materials containing different radionuclides U (Ra), Th, and K. (Ra_{eq}) is calculated based on the equation that 370 Bq/kg of Radium-226, 259 Bq/kg of Thorium-232, or 4810 Bq/kg of Potassium-40 gives an equivalent gamma dose rate [32].

$$Ra_{eq}\ (Bq/kg) = S_{Ra} + 1.43\ S_{Th} + 0.077\ S_k \quad (2)$$

Where S_{Ra}, S_{Th} and S_k is the specific activities in Bq/kg.

Two additional indices are calculated to assess external (H_{ex}) and internal (H_{in}) radiation risks. The determination of H_{ex} is based on the radium equivalent activity with a maximum value of 1, which corresponds to the upper limit of Ra_{eq} (370Bq/kg). These indices should be less than 1 to ensure that the radiation risk remains negligible. H_{ex} is defined as [33,34]:

$$H_{ex} = (S_{Ra}/370) + (S_{Th}/259) + (S_k/4810) \quad (3)$$

The internal hazard index H_{in} was calculated by the equation:

$$H_{in} = (S_{Ra}/185) + (S_{Th}/259) + (S_k/4810) \quad (4)$$

In order to assess external exposure to radionuclides, UNSCEAR (2000) calculated the absorbed dose rates in the open air due to gamma rays in the air at 1 m above the ground. The conversion factors used for this calculation correspond to 0.462 nGy/h for Radium-226, 0.621 nGy/h for Thorium-232 and 0.0417 nGy/h for Potassium-40 per unit activity concentration (Bq/kg) [16,35].

$$D_{air}\ (nGy/h) = 0.462 S_{Ra} + 0.621\ S_{Th} + 0.042 S_k \quad (5)$$

Where S_{Ra}, S_{Th}, and S_k are the activities concentrations of ^{226}Ra, ^{232}Th, and ^{40}K in Bq/kg, respectively.

To determine the annual effective dose rates outdoors, we considered the conversion coefficient of 0.7 Sv/Gy, which converts absorbed dose in air to effective dose. In addition, we used the outdoor occupancy factor of 0.2, as recommended by UNSCEAR (2000). Thus, the annual effective dose rate (mSv/y) was estimated from the formula [36,37]:

$$\text{AED (mSv/y)} = \text{D (nGy/ h)} \times 8760\ \text{h} \times 0.7 \times 10^{-6}\ \text{(Sv/ Gy)} \times 0.2 \quad (6)$$

2.5. Radon concentration measurement

The Alpha GUARD serves as a portable device for assessing the levels of radon concentration in the atmosphere. It is designed to detect air radioactivity by allowing gas diffusion through glass fiber filters in the ionization chamber. This device is appropriate for continuous radon measurements, covering a measurement range of 2.0×10^6 Bq m^{-3} (Alpha GUARD, 2012). For analyzing radon concentration in soil samples, the Alpha GUARD PQ 2000 PRO radon monitors, agricultural soil samples and Alpha pumps are utilized. The levels of radon are monitored every 10 min over a around 180 min. A container with about 300 g of the sample is utilized and this process is repeated multiple times for better accuracy. The flow rate of the pump is set at 0.05 L min^{-1}. An Alpha GUARD monitor is used to measure the radon concentration C_{Rn} (t) as the radon inside the chamber grows. The equilibrium radon concentration (Bq m^{-3}) for samples, which is the constant radon concentration in the enclosed space is evaluated using equation (7),

$$C_{Rn}\ (t)\ (\text{Bq m}^{-3}) = C_{eq}\ (1\text{- exp }(\text{-}\lambda t)) \quad (7)$$

Where the concentrations of radon at time t (Bq m^{-3}) are denoted as C_{Rn} (t), t is the accumulation time of the radon released from the sample [20].

The annual effective dose from inhalation of radon gas (AIED) was calculated to measure the amount of radiation exposure to the lungs from breathing radon gas from the soil using the equation [38]:

$$\text{AIED (mSv/y)} = C_{eq} \times M \times F \times (DCF) \quad (8)$$

Where C_{Rn} is the radon concentration in soil, the equilibrium factor or M is a measure of how well the concentration of radon daughters in air matches the concentration of radon gas and is equal to 0.6. F is the world average outdoor occupation factor (1760 h/y) and the dose conversion factor (DCF) is represented by 9 nSv/Bq h m^{-3}, which means that for each Becquerel of radon per cubic meter of air, adults receive an effective dose of 9 nSv/h to their lungs.

The radon surface exhalation rates and mass exhalation rates for each sample were calculated using the formula given in equations 9 and 10 [20,39].

$$E_a\ \left(\text{Bq m}^{-2}\ \text{s}^{-1}\right) = \frac{C_{eq} \times V \times \lambda}{A} \quad (9)$$

$$E_m\ \left(\text{Bq kg}^{-1}\ \text{s}^{-1}\right) = \frac{C_{eq} \times V \times \lambda}{M} \quad (10)$$

Where V is the volume of the chamber, λ is the decay constant of radon (2.1×10^{-6} s^{-1}), A is the total surface area of the sample, and M is the mass of the sample in kilograms.

3. Results and discussion

The ^{222}Rn activity levels, mass exhalation rates and surface exhalation rates in the soil samples from the Al-Bayda region are presented in Table 1. The ^{222}Rn activities varied from 14 ± 1.6 Bq/m^3 to 255 ± 18 Bq/m^3 with a mean value of 135 ± 15 Bq/m^3, the surface exhalation rates (E_a) ranged from 0.36×10^{-5} to 6.55×10^{-5} Bq $m^{-2}s^{-1}$, with a mean value of 3.46×10^{-5} Bq m^{-2} s^{-1}, while the mass exhalation rate (E_m) varies from 0.17×10^{-7} to 3.21×10^{-7} Bq kg^{-1} s^{-1} with a mean value of 1.69×10^{-7} Bq $kg^{-1}s^{-1}$. The mean ^{222}Rn concentration in the analyzed samples was found to be below the ICRP recommended reference level of 300 Bq/m^3, and the mean surface exhalation rate 3.4 $\times 10^{-5}$ Bq m^{-2} s^{-1} was less than the world limit (0.016 Bq m^{-2} s^{-1}) given by (UNSCEAR, 2000). The rate of radon release should be influenced by the levels of U and Ra present in the soil. However, it is also influenced by several other factors such as permeability, porosity, density and grain size [40].

Table 1
Radon concentration and radon exhalation rate in soil samples collected from Al-Bayda governorate area.

Sample code	C_{eq} (Bq/m^3)	Exhalation rate E_a (Bqm^{-2} s^{-1}) × 10^{-5}	Exhalation rate E_m (Bqkg^{-1} s^{-1}) × 10^{-7}
S1	61 ± 8	1.56 ± 0.14	0.76 ± 0.04
S2	123 ± 12	3.16 ± 0.25	1.54 ± 0.12
S3	230 ± 33	5.91 ± 0.53	2.89 ± 0.29
S4	184 ± 15	4.73 ± 0.51	2.31 ± 0.15
S5	144 ± 11	3.70 ± 0.35	1.81 ± 0.16
S6	109 ± 14	2.80 ± 0.28	1.37 ± 0.17
S7	147 ± 13	3.78 ± 0.48	1.85 ± 0.13
S8	124 ± 15	3.18 ± 0.46	1.56 ± 0.10
S9	142 ± 17	3.63 ± 0.39	1.78 ± 0.11
S10	130 ± 11	3.34 ± 0.47	1.63 ± 0.14
S11	104 ± 10	2.67 ± 0.31	1.31 ± 0.10
S12	237 ± 14	6.09 ± 0.67	2.98 ± 0.21
S13	120 ± 14	3.08 ± 0.29	1.51 ± 0.11
S14	14 ± 1.6	0.36 ± 0.15	0.17 ± 0.09
S15	255 ± 18	6.55 ± 0.68	3.21 ± 0.41
S16	42 ± 1.8	1.085 ± 0.11	0.52 ± 0.54
S17	241 ± 22	6.19 ± 0.74	3.03 ± 0.56
S18	142 ± 19	3.65 ± 0.54	1.78 ± 0.11
S19	128 ± 13	3.29 ± 0.48	1.61 ± 0.13
S20	20 ± 2.6	0.514 ± 0.12	0.25 ± 0.23
Average	135 ± 15	3.46 ± 0.43	1.69 ± 0.12
Min	14	0.36 ± 0.15	0.17 ± 0.09
Max	255	6.55 ± 0.68	3.21 ± 0.41

Table 2 shows the activity concentrations of ^{226}Ra in the soil samples, which ranged from 19.83 ± 1.21 Bq/kg to 36.21 ± 1.35 Bq/kg with a mean value of 27.60 ± 2.40 Bq/kg. The highest concentration of ^{226}Ra was found at sample code (S15) with 36.21 ± 1.35 Bq/kg corresponding to the highest ^{222}Rn concentration at the same location of 255 ± 1.4 Bq/m^3, and the second highest radon level of 241 ± 1.5 Bq/$m^3$is associated with the second highest radium content of 35.34 ± 1.45 Bq/kg found at sample code (S17). Sample code (S14) showed a lower radon concentration compared to others with similar radium content, which means that the correlation between ^{222}Rn and ^{226}Ra activity concentrations in the soil is unclear. In this case, as the soil dries, radon atoms are released from the soil grains as a result of the decay of radium on the mineral surfaces; this release occurs because of the significant kinetic energy (86 keV) possessed by the radon atoms. If the pores are small enough, the radon atoms can escape through them and attach to neighboring grains. Consequently, the ^{222}Rn concentration tends to be low. The correlation between ^{222}Rn concentration and ^{226}Ra activity

Table 2
Activity concentrations of ^{226}Ra, ^{232}Th and ^{40}K (Bq/kg) in soil samples from Al-Bayda area.

Sample code	latitude	Longitude	Activity concentration (Bq/kg)		
			^{226}Ra	^{232}Th	^{40}K
S1	13°58′34.57″N	45°34′34.49″E	24.25 ± 1.24	33.97 ± 1.42	526.33 ± 14
S2	13°58′23.44″N	45°34′26.34″E	24.70 ± 1.58	33.91 ± 1.87	519.97 ± 18
S3	13°58′20.70″N	45°34′26.37″E	35.15 ± 2.5	40.6 ± 2.25	487.88 ± 22
S4	13°58′19.39″N	45°34′27.95″E	31.35 ± 2.1	36.15 ± 1.92	556.19 ± 28
S5	13°58′17.45″N	45°34′25.15″E	26.75 ± 1.9	32.6 ± 1.71	545.68 ± 33
S6	13°58′15.51″N	45°34′22.03″E	25.27 ± 1.5	32.39 ± 2.05	528.58 ± 28
S7	13°58′13.31″N	45°34′24.75″E	27.70 ± 1.6	32.38 ± 1.68	515.63 ± 33
S8	13°58′15.84″N	45°34′15.68″E	26.80 ± 1.5	34.95 ± 1.71	566.36 ± 39
S9	13°58′14.47″N	45°34′6.51″E	25.72 ± 1.45	34.78 ± 2.3	518.57 ± 44
S10	13°58′19.08″N	45°34′37.70″E	27.93 ± 1.8	34.12 ± 2.14	528.01 ± 47
S11	13°58′26.15″N	45°34′50.25″E	23.99 ± 1.8	33.56 ± 2.14	591.07 ± 51
S12	13°58′35.64″N	45°35′10.24″E	30.41 ± 1.75	35.61 ± 1.87	566.14 ± 44
S13	13°58′41.14″N	45°35′23.44″E	24.61 ± 1.8	35.13 ± 1.54	566.05 ± 56
S14	13°58′45.40″N	45°35′35.53″E	28.53 ± 1.63	37.9 ± 2.54	568.02 ± 38
S15	13°58′4.57″N	45°33′45.75″E	36.21 ± 1.35	43.73 ± 2.87	582.02 ± 54
S16	13°59′6.73″N	45°35′38.59″E	23.33 ± 1.78	29.34 ± 1.35	560.57 ± 58
S17	13°59′9.12″N	45°35′25.27″E	35.34 ± 1.45	39.44 ± 2.06	548.01 ± 51
S18	13°59′1.67″N	45°35′54.27″E	28.53 ± 1.4	39.02 ± 2.14	551.28 ± 55
S19	13°59′10.27″N	45°36′43.84″E	26.74 ± 2.1	35.25 ± 2.61	537.77 ± 47
S20	13°59′19.20″N	45°38′23.79″E	19.83 ± 1.21	26.59 ± 1.2	530.12 ± 45
Average			27.60 ± 2.40	35.07 ± 2.45	544.71 ± 48
Min			19.83 ± 1.21	26.59 ± 1.2	487.88 ± 22
Max			36.21 ± 1.35	43.73 ± 2.87	591.07 ± 51

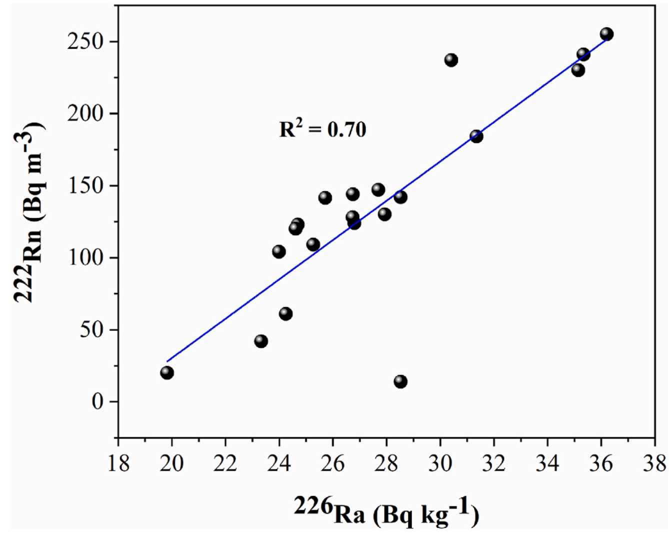

Fig. 2. Correlation between radon and radium concentrations in soil.

concentration in soil samples is shown in Fig. 2, a positive correlation coefficient, $R^2 = 0.70$ is illustrated.

^{232}Th values in the soil samples ranged from 26.59 ± 1.2 Bq/kg to 43.73 ± 2.87 Bq/kg with a mean value of 35.70 ± 2.98 Bq/kg, the maximum value of 43.73 Bq/kg belongs to (S15) site, while the minimum value of 26.74 Bq/kg is related to (S20) site, and for ^{40}K values ranged from 487.88 ± 22 to 591.07 ± 51 Bq/kg with an average value of 544.71 ± 22.18 Bq/kg, the maximum value was 591.07 Bq/kg belongs to (S3) location, while the minimum value of 487.88 Bq/kg is related to (S11) location as shown in Table 2. Table 1 shows that the concentration of ^{226}Ra in all activities of the investigated samples is significantly lower than the global average (33 Bq/kg) reported by (UNSCEAR, 2000), except for sample codes (S3 and S15). For ^{232}Th levels, all samples show lower levels than the world average (40 Bq/kg) reported by UNSCEAR (2000), except for sample code (S15). Also, all samples had values of ^{40}K slightly higher than the world average of 420 Bq/kg [41]. The high ^{40}K activity observed in all samples could be attributed to the agricultural practices in the area and the widespread use of potassium rich fertilizers. The concentrations of ^{232}Th were found to be higher than those of ^{226}Ra in all samples studied, which is consistent with the higher abundance of ^{232}Th radionuclides in the Earth's crust (7.4 μg/g) compared to ^{238}U radionuclides (2.8 μg/g) [41]. Furthermore, the levels of ^{40}K in the soil were observed to be higher than those of ^{226}Ra and ^{232}Th, reflecting the well-known fact that potassium is present in the earth's crust in percentage levels, while uranium and thorium are found at the ppm level [42]. The soil samples examined do not pose a radiological hazard to the population due to the harmful effects of ionizing radiation from the radionuclides in the soil. Fig. 3 (a, b, c)shows the distribution of activity levels for ^{226}Ra, ^{232}Th and ^{40}K in the investigated region. The activity levels of ^{238}U, ^{232}Th, and ^{40}K show an atypical distribution characterized by normal modes. A multivariate statistical method was used to analyze statistical data and generate histograms. IBM SPSS version 21.0, a commercial statistical program, was used for these methods. The Kolmogorov-Smirnov (KS) test was used to determine whether the distribution of results was normal, as shown in Table 3. Since all test p-values were less than 5 %, it can be concluded that the distribution of naturally occurring radionuclide activity in soil samples is normal based on the null hypothesis in the KS test.

The assessment of radiation health risks to both humans and the environment is of paramount importance. These risks are quantified using various parameters such as "radium equivalent activity" (Ra_{eq}), "absorbed dose rate" (D_{air}), "outdoor annual effective dose" (E), and "external and internal hazard index" (H_{ex} and H_{in}), the values of which are given in Table 4. The Ra_{eq} values ranged from 98.67 to 143 Bq/kg with a mean value of 120 Bq/kg, all Ra_{eq} values obtained in the soil samples are below the world limit of 370 Bq/kg [41]. The values of H_{ex} and H_{in} for the investigated samples ranged from 0.28 to 0.38 and from 0.32 to 0.48, respectively, H_{in} and H_{ex} values must be less than one. The absorbed dose rate in nGy/h ranged from 47.282 to 63 nGy/h with a mean of 56.42 nGy/h. The average value of the absorbed dose rate in the investigated soil samples is consistent with the world average value of 59 nGy/h [41]. The average annual effective dose ranges for all samples were 0.05–0.08 with a mean of 0.69 mSv/y, which is consistent with the worldwide limit (0.07 mSv/y) [41]. Thus, our results are in good agreement with those found worldwide. The exposure of the local population in the study area was evaluated by calculating the annual inhalation effective dose (AIED), taking into account the ^{222}Rn levels in the soil surface. The AIED values in the study area ranged from 0.19 to 2.42, with a mean value of 1.28 mSv/y, as shown in Table 4. The results suggest that the mean AIED exposure from radon gas inhalation in the general population is slightly higher than the global annual average effective dose of 1.26 mSv/y given in the UNSCEAR (2000) report and the recommended dose limits of 1 mSv/y set by ICRP.

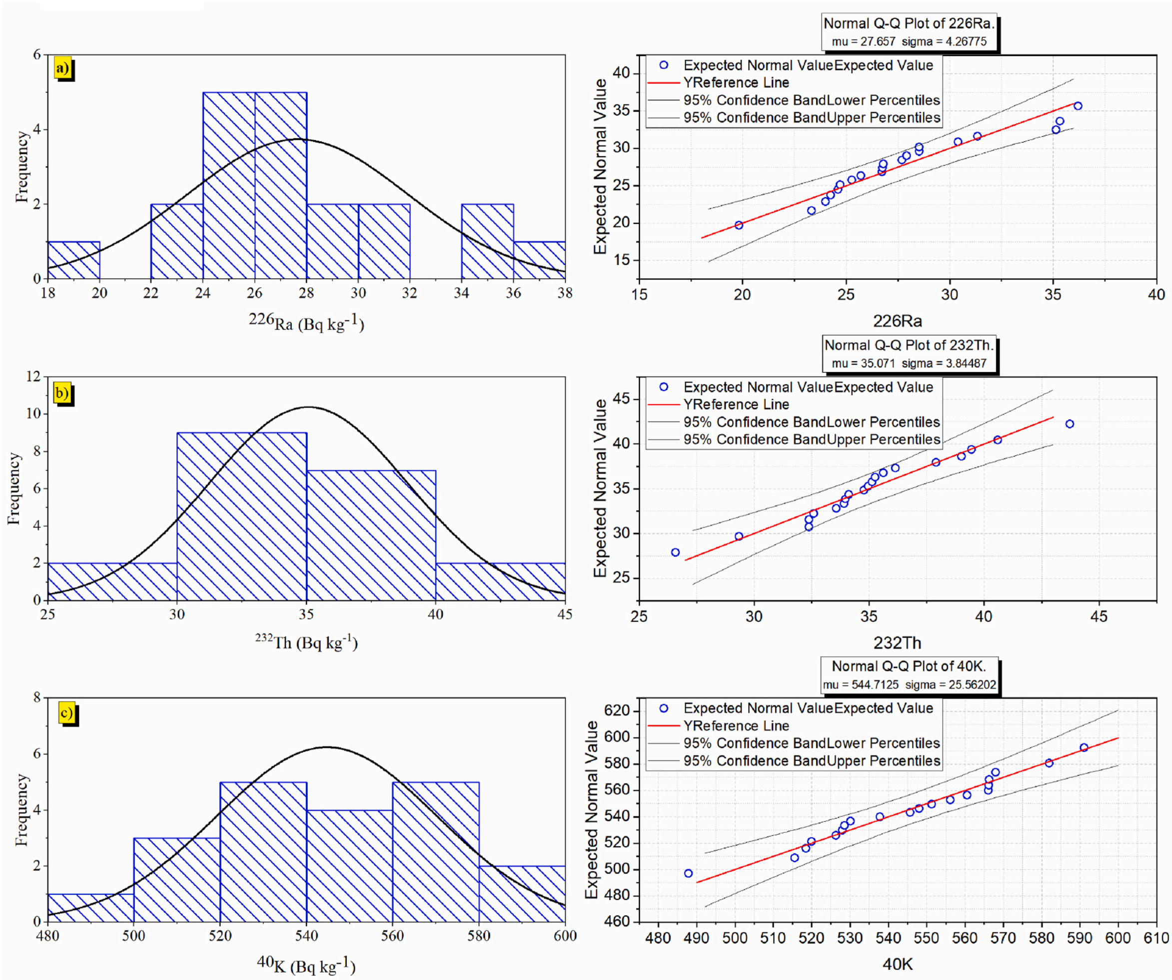

Fig. 3. Frequency distribution analysis and Q–Q plot of ^{226}Ra, ^{232}Th, and ^{40}K in the soil samples from Al-Bayda governorate area.

Table 3
Results of Kolmogorov-Smirnov (KS) normality test.

Radionuclide	Kolmogorov-Smirnov*		
	DF	Statistic	Asymp. Sig. (2 tail)
^{226}Ra	20	0.17	0.57
^{232}Th	20	0.14	0.79
^{40}K	20	0.12	1.00

3.1. Pearson correlation analysis (PC)

In order to find strong relationships and linear correlations between radionuclide levels and radiological risk indicators in soil samples, the study used Pearson correlation analysis. The results showed that the analyzed parameters have different categories based on their linear correlations. The different categories correspond to different degrees of correlation: the first category indicates a low correlation (0.00–0.19), the second category indicates a moderate correlation (0.2–0.39), the third category indicates a significant correlation (0.4–0.79), and the fourth category indicates an incredibly strong correlation (0.8–1.00) [43]. Table 5 lists the correlations between the observed experimental parameters, all of which are positive. The results suggest that the radionuclides found in the samples are naturally occurring and are not influenced by external forces affecting their distribution in the environment. In particular, there is a low correlation between ^{40}K and both ^{226}Ra and ^{232}Th in the investigated soil samples, as well as a significant positive correlation between the activity levels of ^{226}Ra and ^{232}Th

Table 4
Radium equivalent activity, Ra_{eq}, absorbed dose rate (D_{air}), annual effective dose (AED), external hazard index, H_{ex}, and internal hazard index, H_{in}, and annual inhalation effective dose (AED) for soil samples from Al-Bayda area.

Sample code	Ra_{eq} (Bq/Kg)	H_{ex}	H_{in}	D_{air} (nGy/h)	AED	AIED
S1	113.35	0.30	0.37	53.66	0.065	0.57
S2	113.22	0.30	0.37	53.57	0.065	1.16
S3	130.77	0.35	0.44	61.10	0.074	2.18
S4	125.87	0.33	0.42	59.51	0.072	1.74
S5	115.38	0.31	0.38	54.80	0.067	1.36
S6	112.28	0.30	0.37	53.28	0.069	1.03
S7	113.70	0.30	0.38	53.85	0.066	1.39
S8	120.38	0.32	0.39	57.10	0.070	1.17
S9	115.38	0.31	0.38	54.51	0.066	1.34
S10	117.37	0.31	0.39	55.53	0.068	1.23
S11	117.49	0.31	0.38	56.00	0.068	0.98
S12	124.92	0.33	0.41	59.16	0.072	2.25
S13	118.43	0.31	0.38	56.19	0.068	1.14
S14	126.46	0.34	0.41	59.75	0.073	0.133
S15	143.55	0.38	0.48	67.41	0.082	2.42
S16	108.45	0.29	0.35	51.87	0.063	0.399
S17	133.93	0.36	0.45	63.00	0.077	2.29
S18	126.77	0.34	0.41	59.73	0.073	1.34
S19	118.55	0.32	0.39	56.00	0.068	1.21
S20	98.67	0.26	0.32	47.32	0.058	0.19
Average	119.7	0.33	0.39	56.6	0.069	1.28
Min	98.67	0.27	0.32	47.33	0.06	0.28
Max	143.56	0.39	0.49	67.41	0.08	0.41

Table 5
Pearson correlation between natural radionuclides and the radiological hazard coefficients of the soil in the studied area.

	^{226}Ra	^{232}Th	^{40}K	Ra_{eq}	H_{ex}	H_{in}	D_{air}	AED	ELCR
^{226}Ra	1.00								
^{232}Th	0.88	1.00							
^{40}K	0.03	0.16	1.00						
Ra_{eq}	0.93	0.97	0.30	1.00					
H_{ex}	0.93	0.97	0.30	1.00	1.00				
H_{in}	0.96	0.95	0.22	0.99	0.99	1.00			
D_{air}	0.92	0.96	0.34	1.00	1.00	0.99	1.00		
AED	0.92	0.96	0.34	1.00	1.00	0.99	1.00	1.00	
ELCR	0.92	0.96	0.34	1.00	1.00	0.99	1.00	1.00	1.00

(0.88). This suggests that these isotopes are present in the soil under investigation, most likely as a result of natural decay chains. Together with the variables related to radiation hazards, the correlations between ^{226}Ra and ^{232}Th show a consistent pattern. The presence of ^{226}Ra and ^{232}Th in soil samples suggests that these are the main radioactive series sources of radiological hazards and gamma radiation emissions.

3.2. Hierarchical cluster analysis (HCA)

The cluster analysis in this study was performed using Ward's method. Using Ward's method, a relationship can be established between radioactive activity concentrations and radiological parameters, which allows the Euclidean distance separating them to be calculated [44]. Using a dendrogram, Fig. 4 shows two main clusters. ^{226}Ra and ^{232}Th are correlated with the radiological risk markers Ra_{eq}, H_{ex}, H_{in}, D_{air}, AED and ELCR are included in cluster I while ^{40}K is included in cluster II. The results of the Hierarchical Cluster Analysis (HCA) show that there is a significant correlation between soil radioactivity and radium and thorium concentrations. The results are in agreement with the Pearson correlation results.

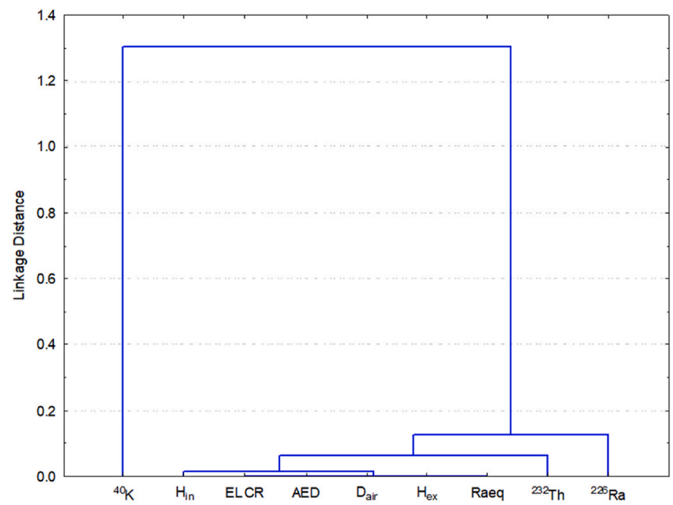

Fig. 4. The clustering analysis of the radiological parameters of the soils in the studied area.

4. Conclusion

The radionuclide contents and radon exhalation rates in soil samples from Albyda area, Yemen were estimated in this work. The results indicate that the mean activities of ^{226}Ra, ^{232}Th don't exceed their corresponding mean activity values recommended by UNSCEAR, except for ^{40}K values which were slightly higher than the permissible limits, the radon concentrations and exhalation rates in soil were within the agreement limit recommended by (ICRP), which is (300 Bq/m^3 and 1.28 mSv/y), and the calculated radiological hazards were also within the world average values. Our results show that all the studied soil samples can be considered safe and do not pose any radiological hazards to the population. Thus, the studied soils are considered suitable for use as agricultural fields and building materials. Multivariate statistical analysis shows a correlation between the calculated radiological parameters and the levels of the studied radionuclides in the soils. This is the first study in which the radioactivity levels and radon exhalation rates in the soil of the Albyda area have been determined, so these results could be used as a data base for a radiological map of this region.

Data availability

The data used to support the finding of this study are available upon request.

CRediT authorship contribution statement

Mohamed Y. Hanfi: Writing – review & editing, Writing – original draft, Visualization, Validation, Supervision, Software, Resources, Project administration, Methodology, Investigation, Funding acquisition, Formal analysis, Data curation, Conceptualization. **Hany El-Gamal:** Writing – review & editing, Writing – original draft, Visualization, Validation, Supervision, Software, Resources, Project administration, Methodology, Investigation, Funding acquisition, Formal analysis, Data curation, Conceptualization. **Maher Taher Hussien:** Writing – review & editing, Writing – original draft, Visualization, Validation, Supervision, Software, Resources, Project administration, Methodology, Investigation, Funding acquisition, Formal analysis, Data curation, Conceptualization. **Mayeen Uddin Khandaker:** Writing – review & editing, Writing – original draft, Visualization, Validation, Supervision, Software, Resources, Project administration, Methodology, Investigation, Funding acquisition, Formal analysis, Data curation, Conceptualization. **Mohammed S. Alqahtani:** Conceptualization, Data curation, Formal analysis, Funding acquisition, Investigation, Methodology, Project administration, Resources, Software, Supervision, Validation, Visualization, Writing – original draft, Writing – review & editing. **Mohamed Hasabelnaby:** Writing – review & editing, Writing – original draft, Visualization, Validation, Supervision, Software, Resources, Project administration, Methodology, Investigation, Funding acquisition, Formal analysis, Data curation, Conceptualization.

Declaration of competing interest

The authors declare that they have no known competing financial interests or personal relationships that could have appeared to influence the work reported in this paper.

Acknowledgments

The authors extend their appreciation to University Higher Education Fund for funding this research work under Research Support Program for Central labs at King Khalid University through the project number CL/PRI/A/7.

References

[1] G. Chambers, D.B. Monabbati, M. Garva, A. Feasby, Naturally occurring radioactive materials, Proc. Am. Gas Assoc. Oper. 1 (2011) 490–502, https://doi.org/10.1201/9780203746042.
[2] M.U. Khandaker, K. Asaduzzaman, A.F. Bin Sulaiman, D.A. Bradley, M.O. Isinkaye, Elevated concentrations of naturally occurring radionuclides in heavy mineral-rich beach sands of Langkawi Island, Malaysia, Mar. Pollut. Bull. 127 (2018) 654–663, https://doi.org/10.1016/j.marpolbul.2017.12.055.
[3] A. El-Taher, A. Al-Turki, Soil - to - Plant Transfer Factors of Naturally Occurring Radionuclides for Selected Plants Growing in Qassim, 2015. Saudi Arabia.
[4] N. Ahmad, M.S. Jaafar, M. Bakhash, M. Rahim, An overview on measurements of natural radioactivity in Malaysia, J. Radiat. Res. Appl. Sci. 8 (2015) 136–141, https://doi.org/10.1016/j.jrras.2014.12.008.
[5] O. Onjun, N. Buasuwan, T. Rungseesumran, N. Kamwang, J. Channuie, P. Sinkaew, Natural rubber block as gamma radiation shielding for medical applications, J. Phys. Conf. Ser. 1285 (2019) 012048, https://doi.org/10.1088/1742-6596/1285/1/012048.
[6] C. Liu, M. Benotto, K. Ungar, J. Chen, Environmental monitoring and external exposure to natural radiation in Canada, J. Environ. Radioact. 243 (2022) 106811, https://doi.org/10.1016/j.jenvrad.2022.106811.
[7] UNSCEAR, SOURCES and EFFECTS of IONIZING RADIATION United Nations Scientific Committee on the Effects of Atomic Radiation, 2010.
[8] V.S. Yakovleva, P.M. Nagorskiy, G.A. Yakovlev, Radon Flux Density soil surf. (2016) 75–82, https://doi.org/10.18454/2313-0156-2016-12-1-75-82.
[9] M. Orabi, Calculating the indoor radon flux from construction materials and soil, Eur. Phys. J. 135 (2020) 1–13, https://doi.org/10.1140/epjp/s13360-020-00483-9.
[10] A. Abbasi, F. Tulucu, N. Almousa, F. Mirekhtiary, H.M.H. Zakaly, The effect of face masks on the filtration rate of Radon (222Rn) gas and its progeny in breathing air, J. Radioanal. Nucl. Chem. 332 (2023) 5017–5022, https://doi.org/10.1007/s10967-023-09209-4.
[11] M.Y.A. Mostafa, M. Vasyanovich, M. Zhukovsky, A primary standard source of radon-222 based on the HPGe detector, Appl. Radiat. Isot. 120 (2017) 101–105, https://doi.org/10.1016/j.apradiso.2016.12.012.
[12] P.V. Pinto, K.S. Kumara, N. Karunakara, Mass exhalation rates, emanation coefficients and enrichment pattern of radon, thoron in various grain size fractions of monazite rich beach placers, Radiat. Meas. (2019) 106220, https://doi.org/10.1016/j.radmeas.2019.106220.
[13] A. Abbasi, F. Mirekhtiary, Estimation of natural gas contribution in indoor 222Rn concentration level in residential houses, J. Radioanal. Nucl. Chem. 330 (2021) 805–810, https://doi.org/10.1007/s10967-021-08024-z.
[14] M.Y.A. Mostafa, M. Vasyanovich, M. Zhukovsky, Prototype of a primary calibration system for measurement of radon activity concentration, Appl. Radiat. Isot. 107 (2016) 109–112, https://doi.org/10.1016/j.apradiso.2015.10.014.
[15] H.N.B. Khalaf, M.Y.A. Mostafa, M. Zhukovsky, A combined system for radioactive aerosol size distribution measurements of radon decay products, Radiat. Phys. Chem. 165 (2019) 108402, https://doi.org/10.1016/j.radphyschem.2019.108402.
[16] UNSCEAR, Sources and effects of ionizing radiation, UNSCEAR 2000 Report to the General Assembly, 2000, pp. 1–10.
[17] A. Abbasi, H.M.H. Zakaly, M.M. Hessien, Radon concentration in compressed natural gas and liquefied petroleum gas and its release range in residential houses, Radiochim. Acta 109 (2021) 793–798, https://doi.org/10.1515/ract-2021-1068.
[18] C. Kranrod, T. Ishikawa, S. Tokonami, A. Sorimachi, S. Chanyotha, N. Chankow, Comparative dosimetry of radon and thoron, Radiat. Protect. Dosim. 141 (2010) 424–427, https://doi.org/10.1093/rpd/ncq233.
[19] IAEA, Safety Reports Series N O . 6 8 Radiation Protection and NORM Residue Management in the Production of Rare Earths from Thorium Containing Minerals, 2012. Vienna.
[20] Y.A. Abdel-Razek, M.S. Masoud, M.Y. Hanafi, M.S. El-Nagdy, Study of the parameters affecting radon gas flux from the stream sediments at Seila area Southeastern desert, Egypt, Environ. Earth Sci. 73 (2015) 8035–8044, https://doi.org/10.1007/s12665-014-3958-2.
[21] M. Hasabelnaby, M.Y. Hanfi, H. El-Gamal, A.H. El Gindy, M.U. Khandaker, G. Salaheldin, The radioactivity levels and beta dose rate assessment from dental ceramic materials in Egypt, Nucl. Eng. Technol. 56 (2024) 3898–3903. https://doi.org/10.1016/j.net.2024.04.036.
[22] M.Y. Hanfi, Radiological assessment of gamma and radon dose rates at former uranium mining tunnels in Egypt, Environ. Earth Sci. 0 (2019), https://doi.org/10.1007/s12665-019-8089-3.
[23] M.Y. Hanfi, B.M. Emad, M.I. Sayyed, M.U. Khandaker, D.A. Bradley, Natural radioactivity in the prospecting tunnel in Egypt: dose rate and risk assessment, Radiat. Phys. Chem. 187 (2021) 109555. https://doi.org/10.1016/j.radphyschem.2021.109555.
[24] S.A, R.K.B. Durrani, Trends in Radiation Dosimetry Solid State Nuclear Track Detection, 1987.
[25] A.Ş. Aykamiş, şeref Turhan, F. Aysun Ugur, U.N. Baykan, A.M. Kiliç, Natural radioactivity, radon exhalation rates and indoor radon concentration of some granite samples usedas construction material in Turkey, Radiat. Protect. Dosim. 157 (2013) 105–111, https://doi.org/10.1093/rpd/nct110.
[26] A. Mohamed, M. Abd El-hady, M. Moustafa, M. Yuness, Deposition pattern of inhaled radon progeny size distribution in human lung, J. Radiat. Res. Appl. Sci. 7 (2014) 333–337, https://doi.org/10.1016/j.jrras.2014.05.004.
[27] ICRP, Compendium of dose coefficients based on ICRP publication 60. https://doi.org/10.1016/j.icrp.2006.06.001, 2012.
[28] K. Suzuki, S. Yamazaki, K. Iwata, Y. Yamada, T. Morioka, K. Daino, M. Kaminishi, M. Ogawa, Y. Shimada, S. Kakinuma, Lung-cancer risk in mice after exposure to gamma rays, carbon ions or neutrons: egfr pathway activation and frequent nuclear abnormality, Radiat. Res. 198 (2022), https://doi.org/10.1667/RADE-21-00192.1.
[29] Y.A. Abdel-Razek, M.S. Masoud, M.Y. Hanfi, M.S. El-Nagdy, Effective radiation doses from natural sources at Seila area South Eastern Desert, Egypt, J. Taibah Univ. Sci. 10 (2016) 271–280. https://doi.org/10.1016/j.jtusci.2015.06.010.
[30] A. Abbasi, Calculation of gamma radiation dose rate and radon concentration due to granites used as building materials in Iran, Radiat. Protect. Dosim. 155 (2013) 335–342, https://doi.org/10.1093/rpd/nct003.
[31] A. Abbasi, Radiation risk assessment of coastal biota from a quasi-Fukushima hypothetical accident in the Mediterranean Sea, Mar. Pollut. Bull. 194 (2023) 115363, https://doi.org/10.1016/j.marpolbul.2023.115363.
[32] Ö. Söğüt, Ö.S. Zorer, H. Reyhanlıoğlu, Radiological hazard assessment of natural gross radioactivity in some cosmetic products, Environ. Forensics 19 (2018) 143–149, https://doi.org/10.1080/15275922.2018.1449036.
[33] Y. Huang, X. Lu, X. Ding, T. Feng, Natural radioactivity level in beach sand along the coast of Xiamen, Mar. Pollut. Bull. (2014), https://doi.org/10.1016/j.marpolbul.2014.11.046.
[34] S. DaPelo, M.M. Aghdam, V. Dentoni, A. Loi, P. Randaccio, Q. Crowley, Assessment of natural radioactivity and radon release potential of silurian black shales, Radiat. Phys. Chem. 215 (2024) 111347, https://doi.org/10.1016/j.radphyschem.2023.111347.
[35] A. Chandrasekaran, R. Ravisankar, G. Senthilkumar, ScienceDirect Spatial distribution and lifetime cancer risk due to gamma radioactivity in Yelagiri Hills , Tamilnadu, Egypt. J. Basic Appl. Sci. (2014) 1–11, https://doi.org/10.1016/j.ejbas.2014.02.001.
[36] S. Monica, P.J. Jojo, M.U. Khandaker, Radionuclide concentrations in medicinal florae and committed effective dose through Ayurvedic medicines, Int. J. Radiat. Biol. 96 (2020) 1028–1037, https://doi.org/10.1080/09553002.2020.1767816.
[37] UNSCEAR, Exposures from natural radiation sources (Annex B), Sources and Effects of Ionizing Radiation, 2000, pp. 84–141, https://doi.org/10.1097/00004032-199907000-00007.
[38] I. Gaafar, M. Hanfi, L.S. El-Ahll, I. Zeidan, Assessment of radiation hazards from phosphate rocks, Sibaiya area, central eastern desert, Egypt, Appl. Radiat. Isot. 173 (2021) 109734, https://doi.org/10.1016/j.apradiso.2021.109734.
[39] G. Salaheldin, A. Tolba, M. Kamel, A. El-Taher, Radiological hazard parameters of natural radionuclides for neoproterozoic rocks from Wadi Um Huytat in central eastern desert of Egypt, J. Radioanal. Nucl. Chem. 325 (2020) 397–408, https://doi.org/10.1007/s10967-020-07262-x.
[40] A. Kumar, S. Kumar, J. Singh, P. Singh, B.S. Bajwa, Journal of Radiation Research and Applied Sciences Assessment of natural radioactivity levels and associated dose rates in soil samples from historical city Panipat , India, J. Radiat. Res. Appl. Sci. 10 (2017) 283–288, https://doi.org/10.1016/j.jrras.2017.05.006.
[41] UNSCEAR, Exposures from Natural Radiation Sources, 2000.
[42] UNSCEAR, United Nations Scientific Committee on the Effects of Atomic Radiation, 1988.
[43] M.J. Abedin, M.R. Karim, M.U. Khandaker, M. Kamal, S. Hossain, M.H.A. Miah, D. A. Bradley, M.R.I. Faruque, M.I. Sayyed, Dispersion of radionuclides from coal-fired brick kilns and concomitant impact on human health and the environment, Radiat. Phys. Chem. 177 (2020) 109165, https://doi.org/10.1016/j.radphyschem.2020.109165.
[44] A.M.A. Adam, M.A.H. Eltayeb, Multivariate statistical analysis of radioactive variables in two phosphate ores from Sudan, J. Environ. Radioact. 107 (2012) 23–43, https://doi.org/10.1016/j.jenvrad.2011.11.021.